

CrossMark  
click for updatesCite this: *Chem. Sci.*, 2016, 7, 2614

# Catenation and encapsulation induce distinct reconstitutions within a dynamic library of mixed-ligand $Zn_4L_6$ cages<sup>†</sup>

Samuel P. Black,<sup>‡a</sup> Daniel M. Wood,<sup>‡a</sup> Felix B. Schwarz,<sup>b</sup> Tanya K. Ronson,<sup>a</sup> Julian J. Holstein,<sup>§ac</sup> Artur R. Stefankiewicz,<sup>¶a</sup> Christoph A. Schalley,<sup>\*b</sup> Jeremy K. M. Sanders<sup>\*a</sup> and Jonathan R. Nitschke<sup>\*a</sup>

Two new  $Zn_4L_6$  cages composed of diamine subcomponents containing either naphthalene diimide (NDI) or porphyrin moieties are described. Their structural differences allow these cages to exhibit distinct interactions with different chemical stimuli, yielding different supramolecular products. The electron-poor NDI subunits of the first cage were observed to thread through electron-rich aromatic crown-ether macrocycles, forming mechanically-interlocked species up to a [3]catenane, whereas the porphyrin ligands of the second cage interacted favourably with  $C_{70}$ , causing it to be bound as a guest. When mixed, the two cages were observed to form a dynamic combinatorial library (DCL) of seven constitutionally distinct mixed-ligand  $Zn_4L_6$  cages. The DCL was observed to reconstitute in opposing ways when treated with either the crown ether or  $C_{70}$ : the electron-rich macrocycle templated the formation of heteroleptic catenanes, whereas  $C_{70}$  caused the DCL to self-sort into homoleptic structures.

Received 19th December 2015

Accepted 21st January 2016

DOI: 10.1039/c5sc04906g

[www.rsc.org/chemicalscience](http://www.rsc.org/chemicalscience)

## Introduction

Living systems respond in complex ways to different stimuli. The study of synthetic chemical systems that reconstitute and respond to different stimuli can offer insight into the signalling events that underpin biological systems,<sup>1</sup> as well as identifying new means to synthesize useful stimuli-responsive systems<sup>2</sup> and materials.<sup>3</sup>

One approach to investigating stimuli-responsive behaviour is to design dynamic combinatorial libraries (DCLs)<sup>4</sup> of molecules that exchange components under thermodynamic control, and thus are inherently responsive to changes in physical conditions and the addition of different stimuli.<sup>5</sup> This

approach has been used to identify protein inhibitors,<sup>6</sup> design mixtures of compounds that self-sort into different host-guest complexes<sup>7</sup> and to engineer separations of mixtures of molecules held together by dynamic covalent bonds.<sup>8</sup> In some cases, the response of a DCL to a stimulus has led, through reconstitution of the system, to the promotion of library members that may otherwise not be observed.<sup>9</sup>

As part of our investigations into stimuli responsive systems, we sought to design an adaptive library of different metallo-supramolecular cages that could respond to templates that are either bound inside the central cavity of a cage,<sup>10</sup> or interact specifically with the edges of an assembly (*i.e.* catenation).<sup>11</sup> To this end, it was necessary to design a library comprised of  $M_4L_6$  cages containing two different kinds of diamine subcomponent, each of which engendered a response to a distinct kind of stimulus. It was also essential that the different ligands in such a library possess near-identical lengths to prevent sterically-driven self-sorting behaviour.<sup>12</sup>

Our DCL is based upon two similarly-sized  $Zn_4L_6$  tetrahedral cages, built using ligands that contain naphthalene diimide (NDI) or Zn-porphyrin moieties, respectively. Combining these cages in solution yielded a DCL of seven different  $Zn_4L_6$  cages, differing in their NDI:porphyrin ligand ratios. By utilizing different molecular recognition events, either the threading of the NDI components through a crown ether, or the encapsulation of the fullerene  $C_{70}$ , we explored the responsive nature of this DCL. The formation of either homoleptic or heteroleptic  $M_4L_6$  structures was favoured, depending on the chemical stimulus that was employed. Our

<sup>a</sup>Department of Chemistry, University of Cambridge, Lensfield Road, Cambridge, CB2 1EW, UK. E-mail: [jkms@cam.ac.uk](mailto:jkms@cam.ac.uk); [jrn34@cam.ac.uk](mailto:jrn34@cam.ac.uk)

<sup>b</sup>Institut für Chemie und Biochemie, Freie Universität Berlin, Takustrasse 3, 14195 Berlin, Germany. E-mail: [c.schalley@fu-berlin.de](mailto:c.schalley@fu-berlin.de)

<sup>c</sup>Global Phasing Ltd., Sheraton House, Castle Park, Cambridge, CB3 0AX, UK

<sup>†</sup> Electronic supplementary information (ESI) available: Full experimental procedures, NMR, ESI-FTICR MS and X-ray crystallography. CCDC 1061975–1061977. For ESI and crystallographic data in CIF or other electronic format see DOI: 10.1039/c5sc04906g

<sup>‡</sup> These authors contributed equally.

<sup>§</sup> Current address: GZG, Department of Crystallography, Georg-August-Universität Göttingen, Goldschmidtstraße 1, 37077 Göttingen, Germany

<sup>¶</sup> Current addresses: Faculty of Chemistry Adam Mickiewicz University, Umultowska 89b, 61-614, Poznań, Poland and Centre for Advanced Technologies, Adam Mickiewicz University, Umultowska 89c, 61-614, Poznań, Poland



study thus represents a singular example of a multi-stimuli-responsive DCL of three-dimensional metallo-supramolecular assemblies. The challenge of analysing and characterising the members of this complex DCL was met by employing electro-spray ionization Fourier-transform ion cyclotron mass spectrometry (ESI-FTICR MS).<sup>13</sup>

## Results and discussion

NDI cage **N**<sub>6</sub> was synthesized through the subcomponent self-assembly<sup>14</sup> of NDI-containing diamine **1** (6 equiv.), 2-formylpyridine (12 equiv.) and zinc triflimide (Zn(NTf<sub>2</sub>)<sub>2</sub>, 4 equiv.) in MeCN (Fig. 1). In similar fashion, Zn-porphyrin cage **P**<sub>6</sub> was prepared using Zn-porphyrin diamine **2** (6 equiv.), 2-formylpyridine (12 equiv.) and zinc triflimide (4 equiv.) in MeCN : CHCl<sub>3</sub> (7 : 3). Both assemblies consisted of Zn<sub>4</sub>L<sub>6</sub> tetrahedra, with the bis(imine) condensation products of 2-formylpyridine and the respective diamine acting as bis-bidentate ligands linking adjacent metal centres.

Cages **N**<sub>6</sub> and **P**<sub>6</sub> were characterised in solution using NMR spectroscopy and ESI-FTICR MS. In both cases, <sup>1</sup>H NMR spectra showed multiple resonances for each proton environment, consistent with the presence of the three possible diastereomers of tetrahedral M<sub>4</sub>L<sub>6</sub> assemblies: homochiral *T* (ΔΔΔΔ/ΛΛΛΛ), heterochiral *C*<sub>3</sub> (ΔΔΔΛ/ΛΛΛΔ), and achiral *S*<sub>4</sub> (ΛΔΔΔ).<sup>15</sup> Analysis of the integrated signal intensities of the <sup>1</sup>H NMR spectrum of **P**<sub>6</sub> indicated a diastereomer distribution of 32 : 48 : 20 (*T* : *C*<sub>3</sub> : *S*<sub>4</sub>) at 298 K (see ESI, Fig. S10†). The diastereomer distribution of **N**<sub>6</sub> could not be determined from its <sup>1</sup>H NMR spectrum (Fig. S3†) due to the greater degree of signal overlap.

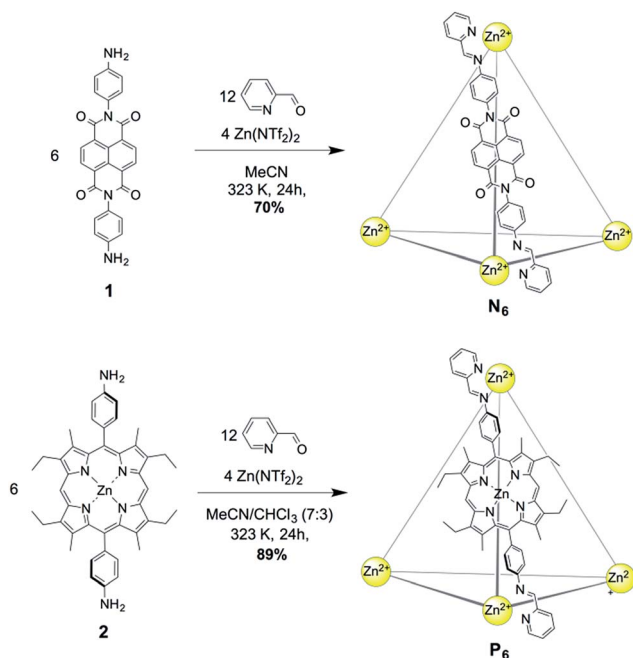


Fig. 1 Synthesis of the Zn<sub>4</sub>L<sub>6</sub> cages **N**<sub>6</sub> (top) from NDI-containing diamine **1**, and **P**<sub>6</sub> (bottom) from Zn-porphyrin containing diamine **2**.

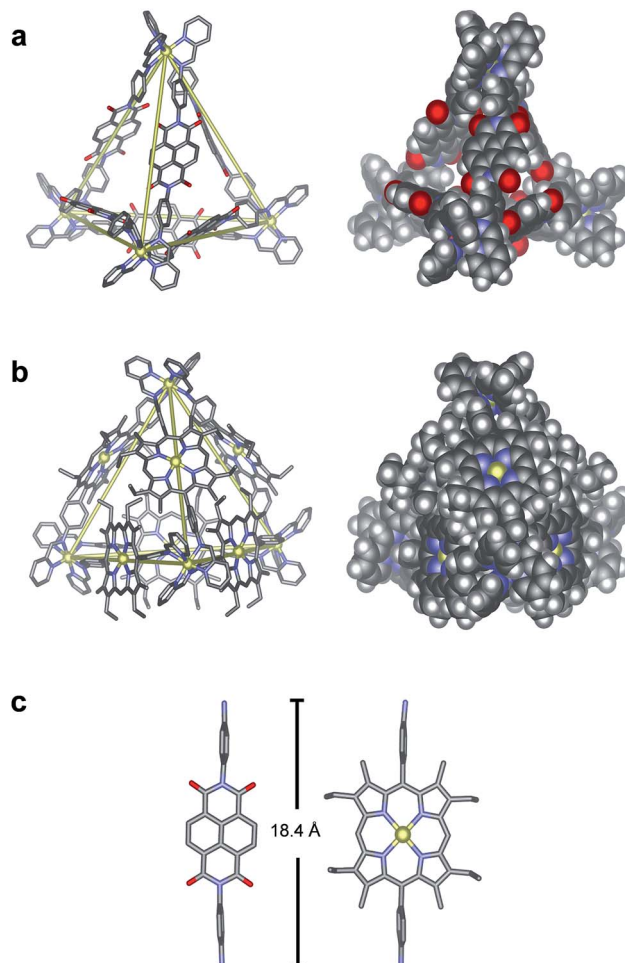


Fig. 2 Crystal structures of Zn<sub>4</sub>L<sub>6</sub> tetrahedra (a) **N**<sub>6</sub> and (b) **P**<sub>6</sub>. Yellow lines connect Zn<sup>II</sup> centres to highlight the tetrahedral frameworks. (c) Comparison of the two diamine residues, highlighting their similar lengths. Hydrogen atoms, disorder, solvent molecules and anions are omitted for clarity. Zn = yellow, C = grey, H = white, N = blue, O = red.

The structures of **N**<sub>6</sub> and **P**<sub>6</sub> were confirmed in the solid state by single-crystal X-ray analysis (Fig. 2). Crystals of **N**<sub>6</sub> were obtained by vapour diffusion of diethyl ether into a solution of **N**<sub>6</sub> in MeCN containing excess KPF<sub>6</sub> (10 equiv.). The crystals were found to contain only the *S*<sub>4</sub>-symmetric diastereomer. Of the six ligands that bridge the four octahedral zinc centres, four thus displayed a *syn*-conformation, bridging zinc centres of opposing handedness, and two adopted an *anti*-conformation, linking zinc centres of identical handedness. The metal–metal separations are 20.6–20.8 Å and 21.0 Å for the *syn*- and *anti*-ligands respectively.

Suitable crystals of **P**<sub>6</sub> were obtained through vapour diffusion of diethyl ether into a solution of its triflate salt in MeCN. In this case, only the *T*-symmetric diastereomer was observed, with both enantiomers (ΔΔΔΔ/ΛΛΛΛ) present in the unit cell. The metal–metal separations range from 20.7–21.4 Å, similar to those observed for **N**<sub>6</sub>. Axial water ligands were observed to bind to three porphyrin–Zn<sup>II</sup> centres, with all three water ligands directed inside the tetrahedral cage (Fig. S32†). The remaining three porphyrin–Zn<sup>II</sup> axial ligands were MeCN molecules that



point outwards from the edges of the tetrahedron. Three of the faces of the  $Zn_4L_6$  tetrahedron are almost completely enclosed by the Zn-porphyrin ligands that define the edges of the assembly. The remaining face is more open due to crystal packing effects, where a corner of each tetrahedron is observed to protrude slightly into the face of another.

Based upon the known affinity of electron-poor NDI moieties for the electron-rich macrocycle bis-1,5-(dinaphtho)-38-crown-10 (C),<sup>16</sup> we anticipated that the NDI edges of cage  $N_6$  would thread through C to yield a library of catenated cages. An excess of C (10 equiv.) was thus added to a  $CD_3CN/CDCl_3$  (1 : 1) solution of  $N_6$ , and the mixture left to equilibrate at 298 K for 24 h. The resultant  $^1H$  NMR spectrum showed the presence of new resonances consistent with C threaded around the NDI groups of  $N_6$  (Fig. S7†), and the ESI-FTICR mass spectrum exhibited signals consistent with  $N_6$  associated with up to four molecules of C (Fig. 3b). In our previously studied system based on a larger NDI-edged tetrahedron, adducts of the cage with up to 12 molecules of C were detected by ESI-FTICR MS. However, infrared multiphoton dissociation (IRMPD) tandem MS analysis demonstrated that the higher adducts were the result of non-specific interactions in the gas phase.<sup>16</sup>

Using a similar approach, the number of catenations per cage between  $N_6$  and C was investigated by IRMPD analysis, in which mass-selected parent ions were irradiated with a  $CO_2$  laser to induce fragmentation (Fig. 4, S19–22†). The  $[Zn_4N_6C(NTf_2)]^{7+}$  and  $[Zn_4N_6C_2(NTf_2)]^{7+}$  ions both underwent symmetrical fragmentation into ‘half-cage’ species  $[Zn_2N_3]^{4+}$  and  $[Zn_2N_3C]^{4+}$ , which further decomposed into smaller fragments (e.g.  $[ZnN]^{2+}$  and  $[ZnNC]^{2+}$ , Fig. 4a–d). When  $[Zn_4N_6C_3(NTf_2)]^{7+}$  was isolated and irradiated,  $[Zn_4N_6C_2(NTf_2)]^{7+}$  (the product of the non-cage-destructive loss of C),  $[Zn_2N_3]^{4+}$  and  $[Zn_2N_3C]^{4+}$  were observed (Fig. 4e and f). Furthermore, the non-

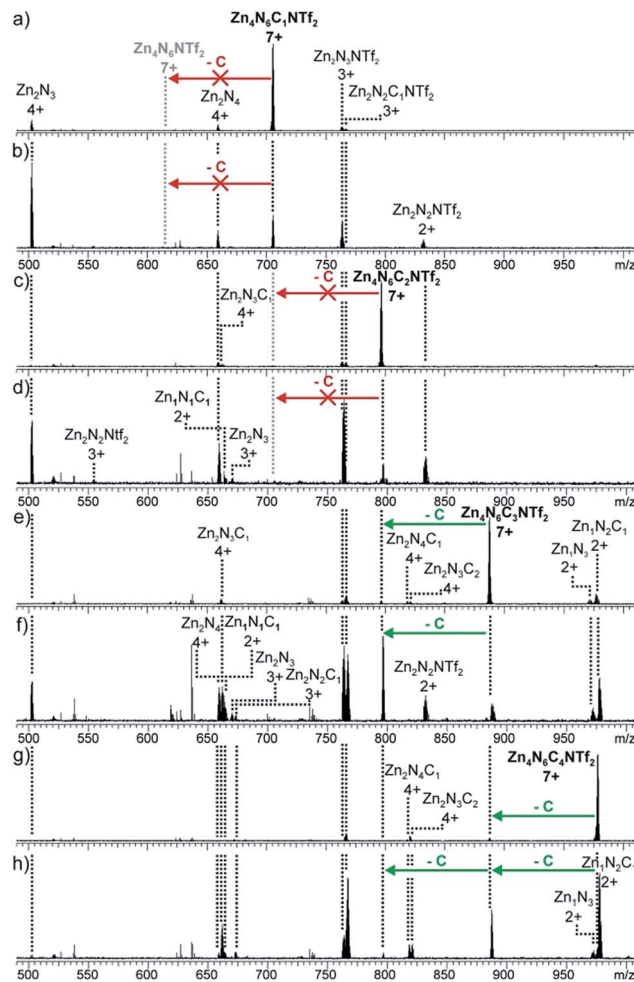


Fig. 4 IRMPD ESI-MS spectra of  $[N_6C_{1-4}NTf_2]^{7+}$  ions. (a)  $N_6C_1$ , 30% laser intensity (b)  $N_6C_1$ , 70% (c)  $N_6C_2$ , 30% (d)  $N_6C_2$ , 50% (e)  $N_6C_3$ , 25% (f)  $N_6C_3$ , 35% (g)  $N_6C_4$ , 20% (h)  $N_6C_4$ , 28%.

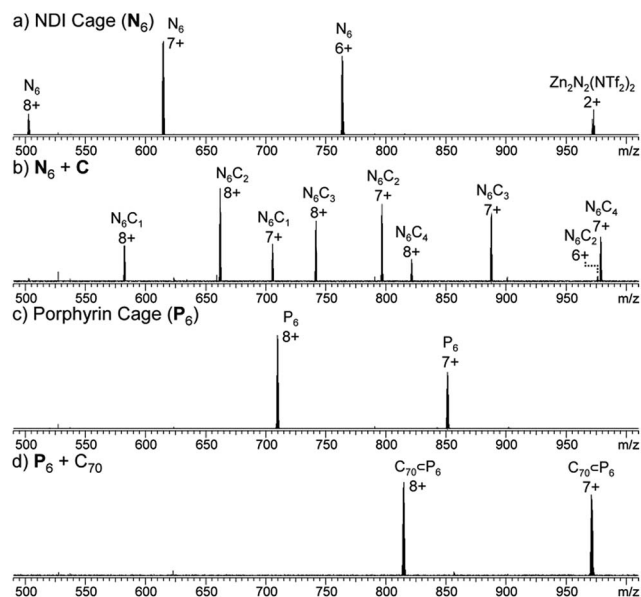


Fig. 3 ESI-MS spectra of (a)  $Zn_4L_6$  NDI cage  $N_6$ , (b)  $N_6 + C$  (4 equiv.), yielding  $N_6C_2$ , (c)  $Zn_4L_6$  porphyrin cage  $P_6$  and (d)  $P_6 + C_{70}$  (5 equiv.), yielding  $C_{70} \subset P_6$ .

symmetric  $[Zn_2N_3C_2]^{4+}$  fragment was not detected, indicating that the  $[Zn_4N_6C_3(NTf_2)]^{7+}$  ion present in the ESI-FTICR mass spectrum does not correspond to a [4]catenane, but results from the non-specific gas-phase interactions between  $N_6C_2$  and C. Similar conclusions can be drawn from the fragmentation of the  $[Zn_4N_6C_4(NTf_2)]^{7+}$  ion, which shows successive loss of two molecules of C without destruction of the cage framework (Fig. 4g and h).

The inhibition of further catenation once two equivalents of C have been threaded onto the  $N_6$  framework contrasts with the statistical non-cooperative binding behaviour observed between C and our previously reported larger NDI-containing tetrahedron. In the larger system, a [7]catenane was obtained, in which up to six molecules of C were threaded onto a tetrahedral framework. The more limited catenation propensity of  $N_6$  appears to arise from its smaller overall size, leading to a sterically-controlled, inhibitive binding process.<sup>17</sup> We postulate that the degree of catenation is limited to two crown ethers, because the binding of a third molecule would require two macrocycles to thread around adjacent NDI ligands, generating steric strain within the resulting assembly.





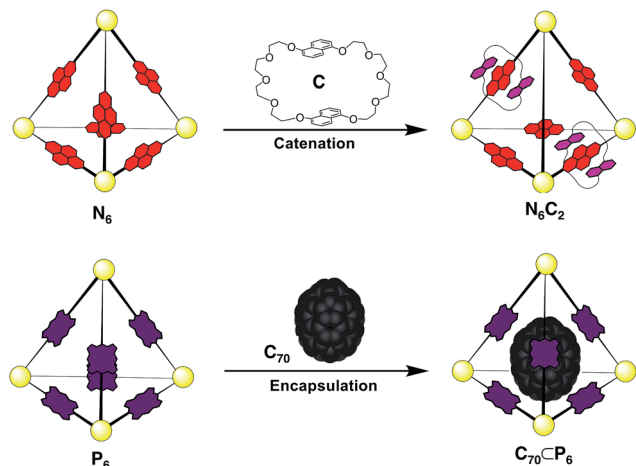


Fig. 5 Summary of the host-guest of the homoleptic cages  $N_6$  and  $P_6$ : catenation of  $N_6$  with crown **C** yielding  $N_6C_2$  (top), encapsulation of fullerene  $C_{70}$  in porphyrin cage  $P_6$ , yielding  $P_6 \subset C_{70}$ , (bottom).

$C_{70}$  was identified as a potential guest molecule for both  $N_6$  and  $P_6$  due to their large internal cavities and the potential for  $\pi$ -interactions between  $C_{70}$  and the ligands of the hosts.<sup>18</sup>  $C_{70}$  (5

equiv.) was thus added to an MeCN solution of either  $N_6$  or  $P_6$  and the mixtures were heated to 323 K for 24 h. Analysis of the mixture of  $N_6$  and  $C_{70}$  provided no evidence for host-guest interaction by either  $^1H$  NMR or ESI-MS. We infer that the large pores in the faces of  $N_6$  provide limited screening of  $C_{70}$  from the bulk solvent; an inner phase is thus not differentiated, in contrast with more enclosed NDI-containing assemblies that have been shown to bind fullerenes.<sup>18a</sup> In contrast, NMR analysis of  $P_6$  after the addition of  $C_{70}$  provided clear evidence of guest binding (Fig. S15†).

The  $^{13}C$  NMR spectrum of the solution showed resonances consistent with the presence of  $C_{70}$ , despite its limited solubility in MeCN. ESI-MS of the solution also showed signals corresponding to the  $C_{70}$  adduct of  $P_6$  (Fig. 3d). We infer from these observations that  $C_{70}$  is encapsulated within the cavity of  $P_6$  (Fig. 5). The behaviour of  $P_6$  contrasted with the analogous porphyrinato- $Ni^{II}$  assembly, which was found to rearrange into new architectures in the presence of  $C_{70}$ .<sup>19</sup> We attribute this differing behaviour to the planar conformation adopted by Zn-porphyrin **2** (as observed in its crystal structure, Fig. 2c and S28†), whereas the Ni-porphyrin congener adopts a saddled conformation.

Having established the responses of  $N_6$  and  $P_6$  to the chemical stimuli of crown **C** and fullerene  $C_{70}$  (Fig. 5), the

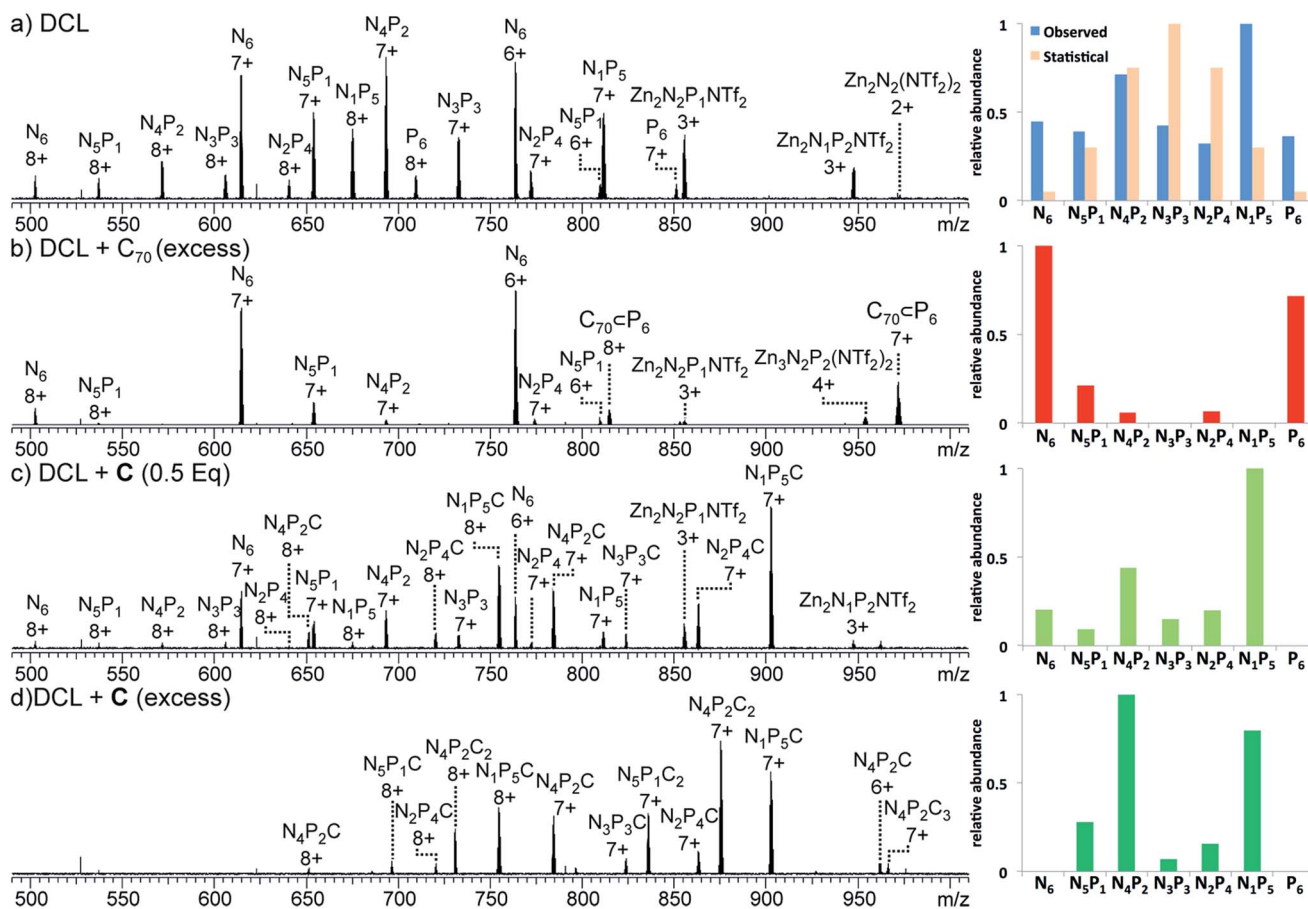


Fig. 6 ESI-MS spectra (left) and corresponding charts (right) that show the relative abundances summed for all observed charge states: (a) 1 : 1 DCL of  $N_6$  and  $P_6$  after 24 h of equilibration, no template, (blue) and statistical distribution (orange) (b) 1 : 1 DCL of  $N_6$  and  $P_6$  containing  $C_{70}$  (4 equiv.), (c) 1 : 1 DCL of  $N_6$  and  $P_6$  with **C** (0.5 equiv.), and (d) 1 : 1 DCL of  $N_6$  and  $P_6$  with **C** (4 equiv.).



responses of a mixed-ligand DCL of tetrahedra were investigated. Separate solutions of pre-formed  $N_6$  and  $P_6$  ( $CD_3CN/CDCl_3$ , 1 : 1, 1.0 mM) were mixed in a 1 : 1 ratio at 298 K. Attempts to confirm the equilibrium state by an independent synthesis from a mixture of all building blocks failed due to incompatible solubilities. As no further changes were observed after 24 hours, we inferred that equilibrium had been reached.

$^1H$  NMR spectra of the mixture showed many resonances, corresponding to the numerous magnetically distinct environments of the mixed-ligand DCL members. The challenge of performing meaningful NMR analysis on this DCL was further complicated by the presence of resonances corresponding to the different regio- and stereo-isomers of the library members. The complicated nature of the spectra rendered DCL analysis by NMR impractical, even with the use of two-dimensional and diffusion-ordered experiments. Therefore, ESI-FTICR MS analysis was employed to gain insight as to the composition of the library. Mass spectra revealed signals which corresponded to all seven of the possible  $Zn_4L_6$  assemblies, hereby labelled  $N_xP_{(6-x)}$  where  $N$  and  $P$  represent the NDI and porphyrin-based ligands (Fig. 6a).

Strictly speaking, a quantitative analysis of the changes in DCL composition using mass spectrometry requires that all species analysed possess similar ESI-response factors.<sup>20</sup> As the homoleptic cages  $N_6$  and  $P_6$  appeared with similar intensities in the mass spectrum of the DCL (Fig. 6a), we infer that this requirement is met to such a degree that changes in peak intensity between mixed ligand species correlate to the degree of change in their solution concentrations in the DCL.<sup>21</sup>

All analysed DCLs were prepared under similar conditions, where solutions of  $N_6$  and  $P_6$  ( $CD_3CN/CDCl_3$ , 1 : 1, 1.0 mM) were allowed to equilibrate over 24 h at 298 K before template addition. The template (C or  $C_{70}$ ) was added to DCLs in excess, at a ratio of 4 : 1 template/cage because this ratio was found to

yield the strongest ESI-MS signals. Following template addition, the library was allowed to equilibrate at room temperature for a further 24 h, by which time no further changes to the library were observed. The MS signals observed in each experiment were processed to establish the relative abundance of each  $N_xP_{(6-x)}$  cage species (summing the detected  $m/z$  signal intensities of the +7 and +8 charge states for each ligand ratio, see the ESI†). In the case of the non-templated DCL (Fig. 6a), each one of the seven possible  $N_xP_{(6-x)}$  species is observed, with  $N_4P_2$  and  $N_1P_5$  occurring in highest abundance.

This distribution deviates from a statistical ratio of species which would follow the 7<sup>th</sup> level of Pascal's triangle (1 : 6 : 15 : 20 : 15 : 6 : 1). We infer this deviation to result from a thermodynamic preference for the homoleptic cages  $N_6$  and  $P_6$ . Minor differences between the lengths of subcomponents 1 and 2 could give rise to slight strain when both ligands are incorporated into the same assembly,<sup>22</sup> thereby favouring the formation of homoleptic over heteroleptic assemblies.<sup>21</sup> Given the high abundance of  $N_1P_5$  observed from a 1 : 1 mixture of  $N_6$  and  $P_6$ , attempts were made to form  $N_1P_5$  exclusively in similar experiments using a 1 : 5 mixture of  $N_6$  and  $P_6$ . These experiments also yielded a  $N_xP_{(6-x)}$  library, which was enriched with  $N_1P_5$ , rather than a single species (Fig. S28†).

Having generated a  $N_xP_{(6-x)}$  DCL, we sought to investigate its response to C and fullerene  $C_{70}$ , which interacted with the individual homoleptic cages  $N_6$  and  $P_6$ , respectively. Following addition of  $C_{70}$  to the DCL and equilibration for 24 h at 298 K (Fig. 6b), the composition shifted to give almost entirely  $N_6$  and  $C_{70} \subset P_6$ . ESI-MS analysis of the library showed that only  $P_6$  was interacting with  $C_{70}$  to form  $C_{70} \subset P_6$ , indicating that this self-sorting behaviour can be attributed to the thermodynamic stability of the  $C_{70} \subset P_6$  host-guest complex, which removes the porphyrin ligands from the system.<sup>23</sup> We observed no evidence

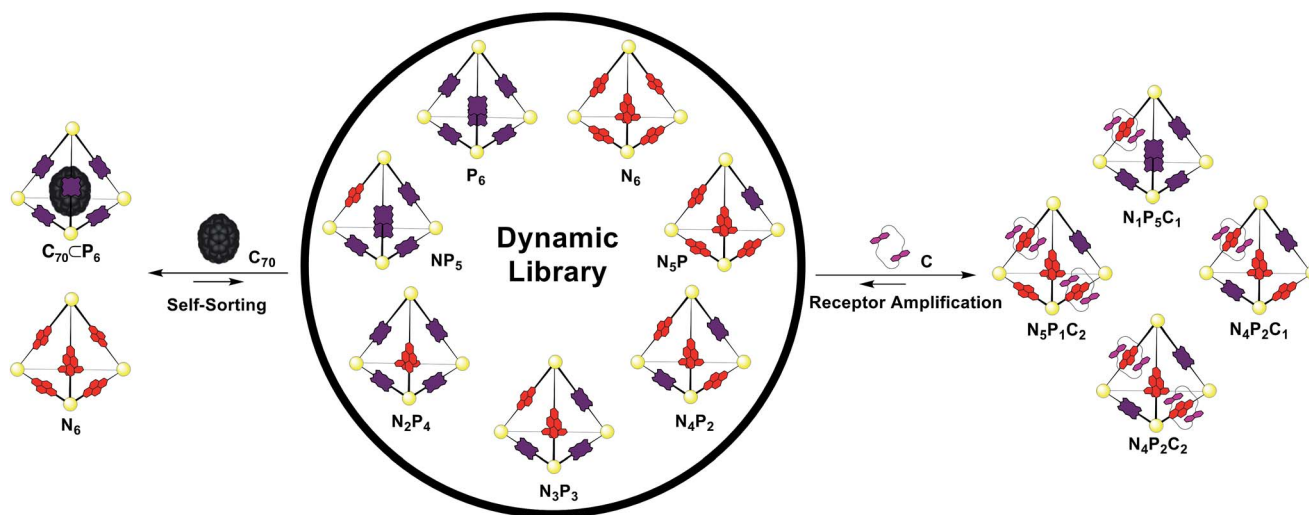


Fig. 7 A schematic overview of the different templation effects observed in the 1 : 1 DCL formed upon mixing of  $N_6$  and  $P_6$ . Addition of  $C_{70}$  leads to the self-sorting of ligands into their homoleptic cages, as the library shifts to form the  $C_{70}$  receptor porphyrin cage  $P_6$ . Addition of macrocycle C leads to the formation of heteroleptic cages, in which the total number of N–C interactions is maximized, given that only two such interactions per cage are possible.



for a mixed-ligand assembly that encapsulates  $C_{70}$ . We infer that the larger surface area of the porphyrin ligands relative to the NDIs (Fig. 2c) renders  $P_6$ , the most enclosed cage, uniquely capable of binding  $C_{70}$ .

While the addition of  $C_{70}$  causes the library distribution to shift almost completely towards the formation of the species with an optimized binding pocket for the template, we anticipated that the addition of  $C$  would have a less pronounced effect on DCL composition. The recognition events of  $C$  are limited to interactions with the NDI components and thus can be expected to affect the library distribution in a way that will maximize the favourable NDI-naphthalene  $\pi$ -interactions.

In the experiment where excess  $C$  (4 equiv.) was added to the  $N_xP_{(6-x)}$  DCL (Fig. 6d), ESI-MS of the equilibrated library showed signals corresponding to mixed ligand assemblies  $N_5P_1$ ,  $N_4P_2$ ,  $N_3P_3$ ,  $N_2P_4$ , and  $N_1P_5$ . These mixed-ligand cages were observed to interact with 1 or 2 units of  $C$ .

No signals for the homoleptic assemblies  $N_6$  or  $P_6$  were observed. Only one signal in the ESI-MS is consistent with a species interacting with three units of  $C$  ( $N_4P_2C_3$ ). Given that this stoichiometry exceeds the degree of catenation previously observed for  $N_6$  (Fig. 4), we infer that the third crown ether is not likely to be catenated.<sup>16,24</sup>

In the similar experiment conducted with a sub-stoichiometric amount of  $C$  (0.5 equiv., Fig. 6c), the ESI-MS shows a distribution of all possible tetrahedral library members except  $P_6$ . In these experiments a maximum of one equivalent of  $C$  was shown to interact with each tetrahedron, and signals were also observed for tetrahedra that are not associated with  $C$ , as expected given the limited amount of  $C$  added in the experiment.

Regardless of the amount of  $C$  added, catenated cages with ligand ratios of  $N_4P_2$  and  $N_1P_5$  were the most abundant species observed in the DCL. This observation follows the trend of speciation in the non-templated DCL, where  $N_4P_2$  and  $N_1P_5$  were also the most abundant library members. However, the addition of  $C$  significantly increases the preference for  $N_4P_2$  and  $N_1P_5$  at the expense of  $N_6$  and  $P_6$  (Fig. 6c and d).

The shift in library composition towards mixed-ligand tetrahedra upon addition of  $C$  appears to maximize the number of interactions between the NDI ligands and  $C$ . In  $N_6$ , a maximum of two molecules of  $C$  can thread the six NDI ligands that are available. Therefore, shifting the library towards mixed-ligand assemblies increases the total number of NDI sites within the system that are available to thread through  $C$ . This hypothesis is supported by the absence of  $N_6$  in the DCL when an excess of  $C$  is present and the observation that all of the species observed by ESI-MS are catenated one or two times.

In order to achieve the maximum degree of catenation between the NDI ligands and  $C$ , the optimal tetrahedra to form are  $N_4P_2$ ,  $N_3P_3$  and  $N_2P_4$  because these species are each able to accommodate two molecules of  $C$  and would thus maximize the number of NDI-naphthalene  $\pi$ -interactions. That  $N_3P_3$  and  $N_2P_4$  are only minor species in the DCL suggests that there are other factors influencing the distribution of the library. This inference is supported by the observation that the non-templated DCL also deviates from the purely statistical distribution, suggesting that the strain leading to a non-statistical distribution of

the non-templated DCL also plays a role in controlling the DCL composition in the presence of  $C$ .

Experiments in which both templates,  $C$  and  $C_{70}$ , were added to the DCL either simultaneously or sequentially yielded poor ESI-MS data. We infer that aggregation may be occurring between  $C$  and  $C_{70}$ , which has been observed in other systems,<sup>25</sup> precluding us from probing possible synergistic effects of these templates upon the DCL.

## Conclusions

The difference in the shape and functionality of the NDI and porphyrin moieties of the ligands of  $N_6$  and  $P_6$  manifests in the form of distinct host-guest interactions with either  $C$  or  $C_{70}$ . The similarity in lengths of the edges of  $N_6$  and  $P_6$  allows for ligand exchange between the two assemblies, yielding a dynamic library of seven different tetrahedral cages  $N_xP_{(6-x)}$ . This DCL was shown to respond to the addition of  $C$  or  $C_{70}$ , with the different templates influencing the composition of the DCL in distinct ways. A point of interest in our study is the use of both encapsulation and catenation (Fig. 7) as templation mechanisms within a DCL of three-dimensional receptors. Unlike systems derived from dynamic covalent species, the labile nature of these  $Zn_4L_6$  tetrahedra precluded analysis by standard chromatographic separation<sup>4b</sup> and instead a methodology was employed where information as to the distribution of the library could be extracted from ESI-MS. This approach allowed us to decipher the behaviour of a complex mixture of seven different cage species, each comprising 22 individual components, and each of which was shown to form additional host-guest interactions. The multiple-stimuli responsiveness thus engendered could be of use in modulating guest uptake within more complex chemical networks that include DCLs of cages.

## Acknowledgements

This work was supported by the UK Engineering and Physical Sciences Research Council (EPSRC), the Deutsche Forschungsgemeinschaft (SFB 765), a Marie Curie Fellowship for J. J. H. (ITN-2010-26465), and a Beilstein-Institut PhD fellowship for F. B. S. We thank Diamond Light Source for synchrotron beamtime on I19 (MT8464).

## Notes and references

- (a) M. Mauro, A. Aliprandi, D. Septiadi, N. S. Kehr and L. De Cola, *Chem. Soc. Rev.*, 2014, **43**, 4144–4166; (b) M. J. Wiester, P. A. Ulmann and C. A. Mirkin, *Angew. Chem., Int. Ed.*, 2011, **50**, 114–137.
- (a) J. T. Foy, D. Ray and I. Aprahamian, *Chem. Sci.*, 2015, **6**, 209–213; (b) D. Ray, J. T. Foy, R. P. Hughes and I. Aprahamian, *Nat. Chem.*, 2012, **4**, 757–762; (c) H. Li, A. C. Fahrenbach, A. Coskun, Z. Zhu, G. Barin, Y. L. Zhao, Y. Y. Botros, J. P. Sauvage and J. F. Stoddart, *Angew. Chem., Int. Ed.*, 2011, **50**, 6782–6788; (d) J. Jo, A. Olsasz, C. H. Chen and D. Lee, *J. Am. Chem. Soc.*, 2013, **135**, 3620–3632; (e)



- J. M. Dragna, G. Pescitelli, L. Tran, V. M. Lynch, E. V. Anslyn and L. Di Bari, *J. Am. Chem. Soc.*, 2012, **134**, 4398–4407.
- 3 (a) J. B. Beck and S. J. Rowan, *J. Am. Chem. Soc.*, 2003, **125**, 13922–13923; (b) K. M. Wong and V. W. Yam, *Acc. Chem. Res.*, 2011, **44**, 424–434; (c) Y. Tidhar, H. Weissman, S. G. Wolf, A. Gulino and B. Rybtchinski, *Chem.–Eur. J.*, 2011, **17**, 6068–6075; (d) T. Mitra, K. E. Jelfs, M. Schmidtman, A. Ahmed, S. Y. Chong, D. J. Adams and A. I. Cooper, *Nat. Chem.*, 2013, **5**, 276–281; (e) L. Motiei, M. Lahav, D. Freeman and M. E. van der Boom, *J. Am. Chem. Soc.*, 2009, **131**, 3468–3469.
- 4 (a) J.-M. Lehn and A. V. Eliseev, *Science*, 2001, **291**, 2331–2332; (b) P. T. Corbett, J. Leclaire, L. Vial, K. R. West, J.-L. Wietor, J. K. M. Sanders and S. Otto, *Chem. Rev.*, 2006, **106**, 3652–3711; (c) F. B. L. Cougnon and J. K. M. Sanders, *Acc. Chem. Res.*, 2012, **45**, 2211–2221; (d) J. Li, P. Nowak and S. Otto, *J. Am. Chem. Soc.*, 2013, **135**, 9222–9239.
- 5 (a) M. E. Belowich and J. F. Stoddart, *Chem. Soc. Rev.*, 2012, **41**, 2003–2024; (b) N. Giuseppone and J.-M. Lehn, *Chem.–Eur. J.*, 2006, **12**, 1715–1722.
- 6 M. Mondal and A. K. H. Hirsch, *Chem. Soc. Rev.*, 2014, **44**, 2455–2488.
- 7 (a) P. Mukhopadhyay, P. Y. Zavalij and L. Isaacs, *J. Am. Chem. Soc.*, 2006, **128**, 14093–14102; (b) A. Wu and L. Isaacs, *J. Am. Chem. Soc.*, 2003, **125**, 4831–4835; (c) F. Wang, C. Han, C. He, Q. Zhou, J. Zhang, C. Wang, N. Li and F. Huang, *J. Am. Chem. Soc.*, 2008, **130**, 11254–11255; (d) S. Dong, X. Yan, B. Zheng, J. Chen, X. Ding, Y. Yu, D. Xu, M. Zhang and F. Huang, *Chem.–Eur. J.*, 2012, **18**, 4195–4199.
- 8 K. Osowska and O. S. Miljanic, *Angew. Chem., Int. Ed.*, 2011, **50**, 8345–8349.
- 9 (a) A. R. Stefankiewicz and J. K. M. Sanders, *Chem. Commun.*, 2013, **49**, 5820–5822; (b) N. Ponnuswamy, F. B. L. Cougnon, G. D. Pantoş and J. K. M. Sanders, *J. Am. Chem. Soc.*, 2014, **136**, 8243–8251; (c) I. A. Riddell, M. M. J. Smulders, J. K. Clegg, Y. R. Hristova, B. Breiner, J. D. Thoburn and J. R. Nitschke, *Nat. Chem.*, 2012, **4**, 751–756.
- 10 (a) S. Lo, J. Lu, L. Krause, D. Stalke, B. Dittrich and G. H. Clever, *J. Am. Chem. Soc.*, 2014, **137**, 1060–1063; (b) M. Han, D. M. Engelhard and G. H. Clever, *Chem. Soc. Rev.*, 2014, **43**, 1848–1860; (c) T. R. Cook and P. J. Stang, *Chem. Rev.*, 2015, **115**, 7001–7045; (d) N. Kishi, M. Akita and M. Yoshizawa, *Angew. Chem., Int. Ed.*, 2014, **53**, 3604–3607; (e) S. Hiraoka, K. Harano, M. Shiro and M. Shionoya, *Angew. Chem., Int. Ed.*, 2005, **44**, 2727–2731.
- 11 (a) K. Ghosh, H. B. Yang, B. H. Northrop, M. M. Lyndon, Y. R. Zheng, D. C. Muddiman and P. J. Stang, *J. Am. Chem. Soc.*, 2008, **130**, 5320–5334; (b) G. Gil-Ramirez, D. A. Leigh and A. J. Stephens, *Angew. Chem., Int. Ed.*, 2015, **54**, 6110–6150.
- 12 (a) A. M. Johnson and R. J. Hooley, *Inorg. Chem.*, 2011, **50**, 4671–4673; (b) C. Gütz, R. Hovorka, G. Schnakenburg and A. Lützen, *Chem.–Eur. J.*, 2013, **19**, 10890–10894; (c) A. Jiménez, R. A. Bilbeisi, T. K. Ronson, S. Zarra, C. Woodhead and J. R. Nitschke, *Angew. Chem., Int. Ed.*, 2014, **53**, 4556–4560.
- 13 A. G. Marshall, C. L. Hendrickson and G. S. Jackson, *Mass Spectrom. Rev.*, 1998, **17**, 1–35.
- 14 (a) T. K. Ronson, S. Zarra, S. P. Black and J. R. Nitschke, *Chem. Commun.*, 2013, **49**, 2476–2490; (b) X.-P. Zhou, Y. Wu and D. Li, *J. Am. Chem. Soc.*, 2013, **135**, 16062–16065; (c) Y. Wu, X.-P. Zhou, J.-R. Yang and D. Li, *Chem. Commun.*, 2013, **49**, 3413–3415; (d) J. Dömer, J. C. Sloatweg, F. Hupka, K. Lammertsma and F. E. Hahn, *Angew. Chem., Int. Ed.*, 2010, **49**, 6430–6433.
- 15 (a) W. Meng, J. K. Clegg, J. D. Thoburn and J. R. Nitschke, *J. Am. Chem. Soc.*, 2011, **133**, 13652–13660; (b) R. W. Saalfrank, B. Demleitner, H. Glaser, H. Maid, D. Bathelt, F. Hampel, W. Bauer and M. Teichert, *Chem.–Eur. J.*, 2002, **8**, 2679–2683; (c) T. Beissel, R. E. Powers, T. N. Parac and K. N. Raymond, *J. Am. Chem. Soc.*, 1999, **121**, 4200–4206.
- 16 S. P. Black, A. R. Stefankiewicz, M. M. J. Smulders, D. Sattler, C. A. Schalley, J. R. Nitschke and J. K. M. Sanders, *Angew. Chem., Int. Ed.*, 2013, **52**, 5749–5752.
- 17 C. A. Hunter and H. L. Anderson, *Angew. Chem., Int. Ed.*, 2009, **48**, 7488–7499.
- 18 (a) A. R. Stefankiewicz, E. Tamanini, G. D. Pantoş and J. K. M. Sanders, *Angew. Chem., Int. Ed.*, 2011, **50**, 5725–5728; (b) D. Canevet, E. M. Pérez and N. Martín, *Angew. Chem., Int. Ed.*, 2011, **50**, 9248–9259; (c) P. D. W. Boyd and C. a. Reed, *Acc. Chem. Res.*, 2005, **38**, 235–242.
- 19 D. M. Wood, W. Meng, T. K. Ronson, A. R. Stefankiewicz, J. K. M. Sanders and J. R. Nitschke, *Angew. Chem., Int. Ed.*, 2015, **54**, 3988–3992.
- 20 E. Leize, A. Jaffrezic and A. V. Dorsselaer, *J. Mass Spectrom.*, 1996, **31**, 537–544.
- 21 P. N. Baxter, R. G. Khoury, J.-M. Lehn, G. Baum and D. Fenske, *Chem.–Eur. J.*, 2000, **6**, 4140–4148.
- 22 M. M. Safont-Sempere, G. Fernandez and F. Würthner, *Chem. Rev.*, 2011, **111**, 5784–5814.
- 23 (a) K. Acharyya and P. S. Mukherjee, *Chem.–Eur. J.*, 2014, **20**, 1646–1657; (b) D. Samanta and P. S. Mukherjee, *Chem.–Eur. J.*, 2014, **20**, 12483–12492; (c) K. Acharyya, S. Mukherjee and P. S. Mukherjee, *J. Am. Chem. Soc.*, 2013, **135**, 554–557; (d) B. H. Northrop, Y. R. Zheng, K. W. Chi and P. J. Stang, *Acc. Chem. Res.*, 2009, **42**, 1554–1563.
- 24 N. Sun, J. Sun, E. N. Kitova and J. S. Klassen, *J. Am. Soc. Mass Spectrom.*, 2009, **20**, 1242–1250.
- 25 S. Bhattacharya, A. Sharma, S. K. Nayak, S. Chattopadhyay and A. K. Mukherjee, *J. Phys. Chem. B*, 2003, **107**, 4213–4217.

